

Synthesis, Spectroscopic, and Structural Studies on Transition Metal Complexes Involving Homoleptic Tripodal Selenoether and Telluroether Coordination

William Levason, Simon D. Orchard, and Gillian Reid*

Department of Chemistry, University of Southampton, Highfield, Southampton SO17 1BJ, U.K.

Received November 16, 1999

The reaction of $[MCl_2(NCMe)_2]$ ($M = Pd$ or Pt) with 2 molar equiv of $MeC(CH_2ER)_3$ ($E = Se$, $R = Me$; $E = Te$, $R = Me$ or Ph) and 2 molar equiv of $TiPF_6$ affords the bis ligand complexes $[M\{MeC(CH_2ER)_3\}_2][PF_6]_2$. The crystal structure of $[Pt\{MeC(CH_2SeMe)_3\}_2][PF_6]_2$ ($C_{16}H_{36}F_{12}P_2PtSe_6$, $a = 12.272(10)$ Å, $b = 18.563(9)$ Å, $c = 15.285(7)$ Å, $\beta = 113.18(3)^\circ$, monoclinic, $P2_1/n$, $Z = 4$) confirms distorted square planar Se_4 coordination at $Pt(II)$, derived from two bidentate tripod selenoethers with the remaining arm not coordinated and directed away from the metal center. Solution NMR studies indicate that these species are fluxional and that the telluroether complexes are rather unstable in solution. The octahedral bis tripod complexes $[Ru\{MeC(CH_2SMe)_3\}_2][CF_3SO_3]_2$ and $[Ru\{MeC(CH_2TePh)_3\}_2][CF_3SO_3]_2$ are obtained from $[Ru(dmf)_6][CF_3SO_3]_3$ and tripod ligand in EtOH solution. The thioether complex ($C_{18}H_{36}F_6O_6RuS_8$, $a = 8.658(3)$ Å, $b = 11.533(3)$ Å, $c = 8.659(2)$ Å, $\alpha = 108.33(2)^\circ$, $\beta = 91.53(3)^\circ$, $\gamma = 106.01(2)^\circ$, triclinic, $P\bar{1}$, $Z = 1$) is isostructural with its selenoether analogue, involving two facially coordinated trithioether ligands in the syn configuration. NMR spectroscopy confirms that this configuration is retained in solution for all of the bis tripod $Ru(II)$ complexes. These low-spin d^6 complexes show unusually high ligand field splittings. The hexaselenoether $Rh(III)$ complex $[Rh\{MeC(CH_2SeMe)_3\}_2][PF_6]_3$ was obtained by treatment of $[Rh(H_2O)_6]^{3+}$ with 2 molar equiv of $MeC(CH_2SeMe)_3$ in aqueous MeOH in the presence of excess PF_6^- anion, while the iridium(III) analogue $[Ir\{MeC(CH_2SeMe)_3\}_2][PF_6]_3$ was obtained via the reaction of the $Ir(I)$ precursor $[IrCl(C_8H_{14})_2]_2$ with the selenoether tripod in MeOH/aqueous HBF_4 . NMR studies reveal different invertomers in solution for both the Rh and Ir species. The $Cu(I)$ complexes $[Cu\{MeC(CH_2ER)_3\}_2]PF_6$ were obtained from $[Cu(NCMe)_4]PF_6$ and tripod ligand in CH_2Cl_2 solution. The corresponding $Ag(I)$ species $[Ag\{MeC(CH_2TeR)_3\}_2]CF_3SO_3$ ($R = Me$ or Ph) were obtained from $Ag[CF_3SO_3]$ and tripod telluroether. In contrast, a similar reaction with 2 molar equiv of $MeC(CH_2SeMe)_3$ afforded only the 1:1 complex $[Ag\{MeC(CH_2SeMe)_3\}]CF_3SO_3$. The structure of this species ($C_9H_{18}AgF_3O_3S_3$, $a = 8.120(3)$ Å, $b = 15.374(3)$ Å, $c = 14.071(2)$ Å, $\beta = 93.86(2)^\circ$, monoclinic, $P2_1/n$, $Z = 4$) reveals a distorted trigonal planar geometry at $Ag(I)$ derived from one bidentate selenoether and one monodentate selenoether. These units are then linked to adjacent $Ag(I)$ ions to give a one-dimensional linear chain cation.

Introduction

Despite the fact that a range of ditelluroether ligands were reported over 10 years ago¹ and thorough investigations into their coordination chemistry have been undertaken, there have been very few reports on the preparation and coordination chemistry of telluroethers of higher denticity. Examples are limited to the tripodal $MeC(CH_2TeR)_3$ ($R = Me$ or Ph), spirocyclic $C(CH_2TePh)_4$, and one recently reported macrocyclic tritelluroether $[12]aneTe_3$ (1,5,9-tritelluracyclododecane).² Indeed, the first coordination compound with a tridentate telluroether *fac*- $[Mn(CO)_3\{MeC(CH_2TeMe)_3\}]CF_3SO_3$ was reported only recently by us,³ reflecting the synthetic difficulties in preparing these sensitive ligands and complexes. We have also reported a detailed investigation into the species *fac*- $[MX(CO)_3(E-E)]$ ($M = Mn$ or Re ; $X = Cl$, Br , or I ; $E-E =$ dithio-, diseleno-, or ditelluroether), probing the relative donating

abilities of group 16 ligands, and we found that, in agreement with the theoretical predictions of Schumann and co-workers,⁴ telluroether ligands are significantly better σ -donors to low-valent metal centers than their lighter analogues.⁵

Previous studies on bidentate telluroethers have concentrated on platinum metal–halide complexes with a 1:1 metal:ditelluroether ratio.⁶ We have recently investigated the coordination chemistry of platinum group metal complexes with a 2:1 ditelluroether:metal ratio, reporting the complexes $[M(L-L)_2][PF_6]_2$ ($M = Pd$ or Pt , $L-L = RTe(CH_2)_3TeR$ ($R = Me$ or Ph) or $o-C_6H_4(TeMe)_2$), $[Rh(L-L)_2Cl_2]PF_6$, $[Ru(L-L)_2X_2]$ ($X = Cl$, Br , or I), and $[Ru(L-L)_2(PPh_3)Cl]PF_6$.⁷ A range of homoleptic copper(I) and silver(I) complexes of the type $[M(E-E)_2]^+$, where $E-E$ is a dithio-, diseleno-, or ditelluroether ligand, have also been reported,^{8,9} the single-crystal X-ray structures of some of which revealed very unusual extended frameworks containing large channels.¹⁰

* Corresponding author address: Department of Chemistry, University of Southampton, Highfield, Southampton SO17 1BJ, U.K.

- (1) Hope, E. G.; Kemmitt, T.; Levason, W. *Organometallics* **1988**, *7*, 78–83.
- (2) Takaguchi, Y.; Horn, E.; Furukawa, N. *Organometallics* **1996**, *15*, 5112–5115.
- (3) Levason, W.; Orchard, S. D.; Reid, G. *J. Chem. Soc., Dalton Trans.* **1999**, 823–824.

(4) Schumann, H.; Arif, A. A.; Rheingold, A. L.; Janiak, C.; Hoffmann, R.; Kuhn, N. *Inorg. Chem.* **1991**, *30*, 1618–1625.

(5) Levason, W.; Orchard, S. D.; Reid, G. *Organometallics* **1999**, *18*, 1275–1280.

(6) Hope, E. G.; Levason, W. *Coord. Chem. Rev.* **1993**, *122*, 109–170.

(7) Levason, W.; Orchard, S. D.; Reid, G.; Tolhurst, V.-A. *J. Chem. Soc., Dalton Trans.* **1999**, 2071–2076.

In light of these results, we are now extending our investigations into the coordination chemistry of tritelluroethers with the hope of establishing whether these ligands are suitable for stabilizing unusual oxidation states and coordination numbers and promoting novel reaction chemistry. We report here the results of a study into the chemistry of the ligands $\text{MeC}(\text{CH}_2\text{-TeR})_3$ ($\text{R} = \text{Me}$ or Ph) and, for comparison, $\text{MeC}(\text{CH}_2\text{SeMe})_3$ with the platinum group and group 11 metals, to form homoleptic species based upon flexible ligands which may allow the metal ion to adopt its preferred coordination geometry. As part of this study, we recently reported the first homoleptic hexaseleno- and hexatelluroether complexes $[\text{Ru}\{\text{MeC}(\text{CH}_2\text{E})_3\}_2][\text{CF}_3\text{SO}_3]_2$ ($\text{E} = \text{Se}$ or Te) along with their electrochemical behavior which suggested that these ligands should be capable of supporting other homoleptic species with a variety of metals.¹¹

Experimental Section

Infrared spectra were measured as CsI disks using a Perkin-Elmer 983 spectrometer over the range 200–4000 cm^{-1} . UV–vis spectra were recorded in solution using 1-cm path-length quartz cells on a Perkin-Elmer Lambda19 spectrometer. Mass spectra were run with positive electrospray (ES^+) using VG Biotech Platform. The ^1H NMR spectra were recorded using a Bruker AM300 spectrometer operating at 300 MHz; $^{77}\text{Se}\{^1\text{H}\}$, $^{125}\text{Te}\{^1\text{H}\}$, and ^{195}Pt NMR spectra were recorded on a Bruker AM360 spectrometer operating at 68.7, 113.6, and 77.4 MHz and referenced to neat Me_2Se , Me_2Te , and aqueous $[\text{PtCl}_6]^{2-}$ ($\delta = 0$), respectively. Microanalyses were performed by the microanalytical service of Strathelyde University. Electrochemical studies used an Eco Chemi PGStat20 device with a 0.1 mol dm^{-3} $n\text{-BuNBF}_4$ supporting electrolyte in MeCN and Pt working and auxiliary electrodes, and they are referenced to a standard calomel reference electrode. All potentials were referenced versus ferrocene-ferrocenium. The complexes $[\text{Cu}(\text{NCMe})_4][\text{PF}_6]_2$,¹² $[\text{IrCl}(\text{C}_8\text{H}_{14})_2]_2$,¹³ and $[\text{Ru}(\text{dmf})_6][\text{CF}_3\text{SO}_3]_3$ ¹⁴ were prepared via the literature procedures, as were the ligands $\text{MeC}(\text{CH}_2\text{-SMe})_3$,¹⁵ $\text{MeC}(\text{CH}_2\text{SeMe})_3$,¹⁶ $\text{MeC}(\text{CH}_2\text{TeMe})_3$,¹ and $\text{MeC}(\text{CH}_2\text{TePh})_3$.¹⁷

$[\text{Pd}\{\text{MeC}(\text{CH}_2\text{SeMe})_3\}_2][\text{PF}_6]_2$. $[\text{PdCl}_2(\text{NCMe})_2]$ (25 mg, 9.6×10^{-5} mol) and TIPF_6 (70 mg, 2.0×10^{-4} mol) were stirred in MeCN (40 cm^3) for 15 min under a dinitrogen atmosphere. $\text{MeC}(\text{CH}_2\text{SeMe})_3$ (68 mg, 1.9×10^{-4} mol) in CH_2Cl_2 (5 cm^3) was then added, and the reaction mixture was stirred at room temperature for 18 h to give a yellow solution and fine white precipitate of TiCl_4 . The solution was filtered to remove the TiCl_4 and reduced to ca. 2 cm^3 in vacuo, and diethyl ether (10 cm^3) was added to precipitate a yellow solid. Yield: 60 mg, 57%. Anal. Calcd for $\text{C}_{16}\text{H}_{36}\text{F}_{12}\text{P}_2\text{PdSe}_6$: C, 17.5; H, 3.3. Found: C, 17.1; H, 3.1. ^1H NMR (CD_3CN): δ 1.34 (s, 1H, CH_3C), 2.41 (s, 3H, SeCH_3), 3.13 (s, 2H, SeCH_2). $^{77}\text{Se}\{^1\text{H}\}$ NMR ($\text{Me}_2\text{CO}/\text{CDCl}_3$, 300 K): δ 110 (br); (220 K) 157, 147 (coordinated SeMe), 32 (uncoordinated SeMe). IR (cm^{-1}): 2940 (w), 2918 (w), 1464 (w), 1405 (sh), 1357 (s), 1272 (w), 1261 (w), 1095 (s), 988 (w), 841 (s), 613 (w), 559 (s). UV–vis (MeCN, cm^{-1} ; ϵ_{mol} , $\text{mol}^{-1} \text{dm}^3 \text{cm}^{-1}$): 26 880 (8420), 33 160 (18 130).

- (8) Black, J. R.; Levason, W. J. *Chem. Soc., Dalton Trans.* **1994**, 3225–3230.
- (9) Black, J. R.; Champness, N. R.; Levason, W.; Reid, G. J. *Chem. Soc., Dalton Trans.* **1995**, 3439–3445.
- (10) Black, J. R.; Champness, N. R.; Levason, W.; Reid, G. *Inorg. Chem.* **1996**, 35, 4432–4438.
- (11) Levason, W.; Orchard, S. D.; Reid, G. J. *Chem. Soc., Chem. Commun.* **1999**, 1071–1072.
- (12) Kubas, G. J. *Inorg. Synth.* **1979**, 19, 90–92.
- (13) Herde, J. L.; Lambert, J. C.; Senoff, C. V. *Inorg. Synth.* **1974**, 15, 18–20.
- (14) Judd, R. J.; Cao, R.; Biner, M.; Armbruster, T.; Burgi, H.-B.; Merbach, A. E.; Ludi, A. *Inorg. Chem.* **1995**, 34, 5080–5083.
- (15) Ali, R.; Higgins, S. J.; Levason, W. *Inorg. Chim. Acta* **1984**, 84, 65–69.
- (16) Gulliver, D. J.; Hope, E. G.; Levason, W.; Marshall, G. L.; Murray, S. G.; Potter, D. M. *J. Chem. Soc., Perkin Trans. 2* **1984**, 429–434.
- (17) Connolly, J. C.; Genge, A. R. J.; Levason, W.; Orchard, S. D.; Pope, S. J. A.; Reid, G. J. *Chem. Soc., Dalton Trans.* **1999**, 2343–2351.

$[\text{Pd}\{\text{MeC}(\text{CH}_2\text{TeMe})_3\}_2][\text{PF}_6]_2$ was prepared similarly to give a brown solid (38%). Anal. Calcd for $\text{C}_{16}\text{H}_{36}\text{F}_{12}\text{P}_2\text{PdTe}_6$: C, 13.8; H, 2.6. Found: C, 13.1; H, 2.3. ^1H NMR (CD_3CN): δ 1.39 (s, 1H, CH_3C), 2.35 (s, 3H, TeCH_3), 3.15 (s, 2H, TeCH_2). IR (cm^{-1}): 2940 (w), 1356 (s), 1092 (s), 988 (m), 838 (s), 613 (w), 557 (m). UV–vis (MeCN, cm^{-1} ; ϵ_{mol} , $\text{mol}^{-1} \text{dm}^3 \text{cm}^{-1}$): 24 650 (sh, 4970), 29 800 (sh, 10 280), 36 870 (18 300).

$[\text{Pd}\{\text{MeC}(\text{CH}_2\text{TePh})_3\}_2][\text{PF}_6]_2$ was prepared similarly to give an orange solid (65%). Anal. Calcd for $\text{C}_{46}\text{H}_{48}\text{F}_{12}\text{P}_2\text{PdTe}_6$: C, 31.3; H, 2.5. Found: C, 31.3; H, 2.5. ^1H NMR (CD_3CN): δ 1.33 (s, 1H, CH_3C), 3.33 (s, 2H, TeCH_2), 7.30–7.55 (m, 5H, TePh). $^{125}\text{Te}\{^1\text{H}\}$ NMR ($\text{Me}_2\text{CO}/\text{CDCl}_3$, 190 K): δ 561, 528. IR (cm^{-1}): 3061 (w), 1570 (w), 1476 (w), 1434 (w), 1359 (s), 1267 (w), 1096 (s), 1024 (w), 997 (m), 837 (s), 733 (m), 690 (m), 613 (w), 558 (m), 453 (m). UV–vis (MeCN, cm^{-1} ; ϵ_{mol} , $\text{mol}^{-1} \text{dm}^3 \text{cm}^{-1}$): 26 940 (19 510), 37 650 (sh, 23 160).

$[\text{Pt}\{\text{MeC}(\text{CH}_2\text{SeMe})_3\}_2][\text{PF}_6]_2$. PtCl_2 (25 mg, 9.4×10^{-5} mol) was refluxed in MeCN for 2 h to give a light yellow solution of $[\text{PtCl}_2(\text{NCMe})_2]$. TIPF_6 (66 mg, 1.9×10^{-4} mol) and $\text{Me}(\text{CH}_2\text{SeMe})_3$ (68 mg, 1.9×10^{-4} mol) in CH_2Cl_2 (5 cm^3) were then added, and the reaction mixture was stirred at room temperature for 48 h to give a yellow solution and a fine white precipitate of TiCl_4 . The solution was filtered to remove the TiCl_4 and reduced to ca. 2 cm^3 in vacuo, and diethyl ether (10 cm^3) was added to precipitate a pale yellow solid. Yield: 56 mg, 50%. Anal. Calcd for $\text{C}_{16}\text{H}_{36}\text{F}_{12}\text{P}_2\text{PtSe}_6$: C, 16.2; H, 3.0. Found: C, 15.9; H, 3.1. ^1H NMR (CD_3CN): δ 1.33 (s, 1H, CH_3C), 2.48 (s, 3H, SeCH_3), 3.25 (s, 2H, SeCH_2). $^{77}\text{Se}\{^1\text{H}\}$ NMR ($\text{Me}_2\text{CO}/\text{CDCl}_3$, 300 K): δ 144 (br); (220 K) 141.8, 142.6, 149.5, 150.3 (coordinated SeMe), 33.7 (uncoordinated SeMe). ^{195}Pt NMR ($\text{Me}_2\text{CO}/\text{CDCl}_3$, 220 K): δ -4630, -4888. IR (cm^{-1}): 2951 (w), 2918 (w), 1405 (sh), 1357 (m), 1095 (m), 986 (w), 834 (s), 613 (w), 559 (s). UV–vis (MeCN, cm^{-1} ; ϵ_{mol} , $\text{mol}^{-1} \text{dm}^3 \text{cm}^{-1}$): 28 500 (1300), 33 560 (6310).

$[\text{Pt}\{\text{MeC}(\text{CH}_2\text{TeMe})_3\}_2][\text{PF}_6]_2$ was prepared similarly to give a brown solid (28%). Anal. Calcd for $\text{C}_{16}\text{H}_{36}\text{F}_{12}\text{P}_2\text{PtTe}_6$: C, 13.0; H, 2.4. Found: C, 13.4; H, 2.2. ^1H NMR (CD_3CN): δ 1.39 (s, 1H, CH_3C), 2.26 (s, 3H, TeCH_3), 3.27 (s, 2H, TeCH_2). IR (cm^{-1}): 2929 (w), 2895 (w), 1358 (s), 1097 (s), 991 (m), 836 (s), 613 (w), 558 (m). UV–vis (MeCN, cm^{-1} ; ϵ_{mol} , $\text{mol}^{-1} \text{dm}^3 \text{cm}^{-1}$): 30 560 (sh, 8630), 36 870 (20 350).

$[\text{Pt}\{\text{MeC}(\text{CH}_2\text{TePh})_3\}_2][\text{PF}_6]_2$ was prepared similarly to give an orange solid (20%). Anal. Calcd for $\text{C}_{46}\text{H}_{48}\text{F}_{12}\text{P}_2\text{PtTe}_6$: C, 29.8; H, 2.6. Found: C, 29.8; H, 2.4. ^1H NMR (CD_3CN): δ 1.30 (s, 1H, CH_3C), 3.42 (s, 2H, TeCH_2), 7.35–7.55 (m, 5H, TePh). $^{125}\text{Te}\{^1\text{H}\}$ NMR ($\text{Me}_2\text{CO}/\text{CDCl}_3$, 190 K): δ 547, 542, 518, 512 (coordinated TePh), 395 (uncoordinated TePh). IR (cm^{-1}): 3017 (w), 1572 (w), 1474 (w), 1435 (w), 1359 (s), 1267 (w), 1096 (s), 997 (m), 836 (s), 734 (m), 690 (m), 613 (w), 557 (s), 453 (m). UV–vis (MeCN, cm^{-1} ; ϵ_{mol} , $\text{mol}^{-1} \text{dm}^3 \text{cm}^{-1}$): 32 050 (19 360), 37 760 (sh, 32 350).

$[\text{Ru}\{\text{MeC}(\text{CH}_2\text{SMe})_3\}_2][\text{CF}_3\text{SO}_3]_2$. $[\text{Ru}(\text{dmf})_6][\text{CF}_3\text{SO}_3]_3$ (70 mg, 7.1×10^{-5} mol) was added to a solution of $\text{MeC}(\text{CH}_2\text{SeMe})_3$ (33 mg, 1.6×10^{-4} mol) in MeOH (40 cm^3). The reaction mixture was refluxed under an atmosphere of dinitrogen for 24 h to give a yellow solution. Reduction of the solvent volume in vacuo to 1 cm^3 and the addition of a diethyl ether gave a light yellow solid. Yield: 40 mg, 69%. Anal. Calcd for $\text{C}_{18}\text{H}_{36}\text{F}_6\text{O}_6\text{RuS}_8$: C, 26.4; H, 4.4. Found: C, 26.0; H, 4.1. ^1H NMR (CD_3CN): δ 1.28 (s, 1H, CH_3C), 2.47 (s, 3H, SCH_3), 2.85 (s, 2H, SCH_2). ES^+ (MeCN) m/z : 671, 261; calcd for $[\text{Ru}\{\text{MeC}(\text{CH}_2\text{SMe})_3\}_2][\text{CF}_3\text{SO}_3]^+$ 671, $[\text{Ru}\{\text{MeC}(\text{CH}_2\text{SMe})_3\}_2]^{2+}$ 261. IR (cm^{-1}): 2984 (w), 2940 (w), 1463 (w), 1423 (m), 1358 (w), 1262 (s), 1227 (m), 1167 (m), 1151 (m), 1097 (w), 1032 (s), 976 (m), 874 (w), 812 (w), 756 (w), 721 (w), 639 (s), 573 (w), 518 (m), 429 (w). UV–vis (MeCN, cm^{-1} ; ϵ_{mol} , $\text{mol}^{-1} \text{dm}^3 \text{cm}^{-1}$): 27 530 (160), 31 730 (180), 35 210 (1990), 43 480 (18 590).

$[\text{Ru}\{\text{MeC}(\text{CH}_2\text{SeMe})_3\}_2][\text{CF}_3\text{SO}_3]_2$ was prepared similarly to give a yellow solid (42%). Anal. Calcd for $\text{C}_{18}\text{H}_{36}\text{F}_6\text{O}_6\text{RuS}_2\text{Se}_6$: C, 19.6; H, 3.3. Found: C, 19.9; H, 3.2. ^1H NMR (CD_3NO_2): δ 1.46 (s, 1H, CH_3C), 2.51 (s, 3H, SeCH_3), 2.6–2.9 (br, 2H, SeCH_2). $^{77}\text{Se}\{^1\text{H}\}$ NMR ($\text{MeNO}_2/\text{CDCl}_3$, 300 K): δ 120.2. ES^+ (MeCN) m/z : 953, 403; calcd for $[\text{Ru}\{\text{MeC}(\text{CH}_2\text{SeMe})_3\}_2][\text{CF}_3\text{SO}_3]^+$ 959, $[\text{Ru}\{\text{MeC}(\text{CH}_2\text{SeMe})_3\}_2]^{2+}$ 405. IR (cm^{-1}): 1461 (w), 1416 (w), 1359 (m), 1261 (s), 1227 (m), 1167 (m), 1151 (m), 1099 (w), 1032 (s), 921 (m),

897 (m), 834 (w), 757 (w), 639 (s), 573 (m), 518 (m). UV-vis (MeCN, cm^{-1} ; ϵ_{mol} , $\text{mol}^{-1} \text{ dm}^3 \text{ cm}^{-1}$): 25 930 (220), 29 900 (230), 39 800 (38 230).

[Ru{MeC(CH₂TeMe)₃}₂][CF₃SO₃]₂ was prepared similarly to give a brown solid (33%). Anal. Calcd for C₁₈H₃₆F₆O₆RuS₂Te₆: C, 15.5; H, 2.6. Found: C, 15.2; H, 2.7. ¹H NMR (CD₃NO₂): δ 1.71 (s, 1H, CH₃C), 2.38 (s, 3H, TeCH₃), 2.5–2.7 (br, 2H, TeCH₂). ¹²⁵Te{¹H} NMR (MeNO₂/CDCl₃, 300 K): δ 204. ES⁺ (MeCN) *m/z*: 547; calcd for [¹⁰²Ru{MeC(CH₂¹³⁰TeMe)₃}₂]²⁺ 555. IR (cm⁻¹): 2962 (w), 2907 (w), 1360 (s), 1271 (s), 1232 (sh), 1161 (m), 1095 (m), 1032 (m), 834 (m), 759 (w), 639 (s), 616 (sh), 574 (w), 517 (m). UV-vis (MeCN, cm^{-1} ; ϵ_{mol} , $\text{mol}^{-1} \text{ dm}^3 \text{ cm}^{-1}$): 26 890 (sh, 2450), 35 800 (22 000), 41 800 (28 100).

[Ru{MeC(CH₂TePh)₃}₂][CF₃SO₃]₂ was prepared similarly to give a brown solid (49%). Anal. Calcd for C₄₈H₄₈F₆O₆RuS₂Te₆: C, 32.6; H, 2.7. Found: C, 32.2; H, 2.8. ¹H NMR (CD₃CN): δ 1.67 (s, 3H, CH₃C), 2.5–3.6 (br, 6H, TeCH₂), 7.2–7.6 (m, 15H, TePh). ¹²⁵Te{¹H} NMR (MeNO₂/CDCl₃, 300 K): δ 481. ES⁺ (MeCN) *m/z*: 734; calcd for [¹⁰²Ru{MeC(CH₂¹³⁰TePh)₃}₂]²⁺ 741. IR (cm⁻¹): 2918 (w), 1570 (w), 1476 (w), 1432 (w), 1359 (s), 1278 (s), 1258 (s), 1160 (m), 1085 (m), 1030 (s), 996 (m), 835 (w), 738 (s), 690 (m), 637 (s), 517 (m), 453 (m). UV-vis (MeCN, cm^{-1} ; ϵ_{mol} , $\text{mol}^{-1} \text{ dm}^3 \text{ cm}^{-1}$): 25 720 (1330), 32 720 (29 000), 35 310 (33 990).

[Rh{MeC(CH₂SeMe)₃}₂][PF₆]₃. AgNO₃ (56 mg, 3.3 × 10⁻⁴ mol) was added to a solution of RhCl₃·3H₂O (29 mg, 1.1 × 10⁻⁴ mol) in H₂O (15 cm³), and the mixture was refluxed for 2 h. The AgCl was filtered off to leave a yellow solution, to which was added MeC(CH₂SeMe)₃ (78 mg, 2.2 × 10⁻⁴ mol) in MeOH (25 cm³), and the mixture was refluxed for 24 h. Addition of NH₄PF₆ (65 mg, 4.0 × 10⁻⁴ mol) gave a fine purple precipitate. Yield: 45 mg, 33%. Anal. Calcd for C₁₆H₃₆F₁₈P₃RhSe₆: C, 15.5; H, 2.9. Found: C, 16.0; H, 2.6. ¹H NMR (CD₃CN): δ 1.40 (s, 1H, CH₃C), 2.39 (s), 2.49 (s), 2.54 (s), 2.61 (s, 3H, SeCH₃), 2.80–2.85 (br, 2H, SeCH₂). ⁷⁷Se{¹H} NMR (MeNO₂/CDCl₃, 300 K): δ 117.3, 134.8, 147.5, 152.1. ⁷⁷Se{¹H} NMR (200 K, ¹J in parentheses): δ 126.2 (d, 43 Hz), 136.6 (d, 42 Hz), 137.2 (d, 43 Hz), 155.3 (d, 43 Hz), 159.0 (d, 42 Hz). ES⁺ (MeCN) *m/z*: 395; calcd for [¹⁰³Rh{MeC(CH₂⁸⁰SeMe)₃}₂]{MeC(CH₂⁸⁰SeMe)₂(CH₂⁸⁰Se)}]²⁺ 398. IR (cm⁻¹): 2963 (w), 1460 (w), 1358 (s), 1264 (w), 1096 (s), 988 (m), 836 (s), 743 (w), 671 (w), 614 (m), 558 (s). UV-vis (MeCN, cm^{-1} ; ϵ_{mol} , $\text{mol}^{-1} \text{ dm}^3 \text{ cm}^{-1}$): 21 180 (1720), 32 570 (62 200), 39 060 (68 110).

[Ir{MeC(CH₂SeMe)₃}₂][PF₆]₃. [IrCl(C₈H₁₄)₂]₂ (34 mg, 3.8 × 10⁻⁵ mol) was added to MeC(CH₂SeMe)₃ (62 mg, 1.8 × 10⁻⁴ mol) and 40% HBF₄ (0.5 cm³) in a mixture of water (20 cm³) and methanol (10 cm³), and the reaction mixture was refluxed for 18 h to give a yellow solution. After the mixture had been cooled, excess NH₄PF₆ (59 mg, 3.6 × 10⁻⁴ mol) was added, and the solvent was removed in vacuo. The residue was dissolved in MeNO₂ (5 cm³) and filtered, and diethyl ether (20 cm³) was added to give a light yellow precipitate. Yield: 55 mg, 46%. Anal. Calcd for C₁₆H₃₆F₁₈P₃IrSe₆: C, 14.5; H, 2.7. Found: C, 14.0; H, 2.5. ¹H NMR (CD₃CN): δ 1.35 (s, 1H, CH₃C), 2.44–2.60 (m, 3H, SeCH₃), 2.80–3.05 (br, 2H, SeCH₂). ⁷⁷Se{¹H} NMR (MeNO₂/CDCl₃, 300 K): δ 77.6, 87.4, 109.1. ES⁺ (MeCN) *m/z*: 439; calcd for [¹⁹³Ir{MeC(CH₂⁸⁰SeMe)₃}₂]{MeC(CH₂⁸⁰SeMe)₂(CH₂⁸⁰Se)}]²⁺ 443. IR (cm⁻¹): 2929 (w), 1359 (s), 1087 (s), 839 (s), 557 (m). UV-vis (MeCN, cm^{-1} ; ϵ_{mol} , $\text{mol}^{-1} \text{ dm}^3 \text{ cm}^{-1}$): 40 850 (19 250), 45 290 (23 150).

[Cu{MeC(CH₂SeMe)₃}₂][PF₆]₂. [Cu(NCMe)₄][PF₆]₂ (37 mg, 9.9 × 10⁻⁵ mol) was added to a solution of MeC(CH₂SeMe)₃ (75 mg, 2.1 × 10⁻⁴ mol) in dry CH₂Cl₂ (35 cm³). The reaction mixture was stirred for 1 h and refluxed for 10 min. After the mixture had been cooled, the solvent volume was reduced in vacuo to 5 cm³, and diethyl ether (15 cm³) was added to give a pale yellow solid. Yield: 74 mg, 82%. Anal. Calcd for C₁₆H₃₆CuF₆PSe₆·CH₂Cl₂: C, 20.5; H, 3.8. Found: C, 19.9; H, 3.7. ¹H NMR (CDCl₃): δ 1.25 (s, 1H, CH₃C), 2.22 (s, 3H, SeCH₃), 2.88 (s, 2H, SeCH₂). ES⁺ (MeCN) *m/z*: 456, 415; calcd for [⁶³Cu{MeC(CH₂⁸⁰SeMe)₃}₂](NCMe)]⁺ 458, [⁶³Cu{MeC(CH₂⁸⁰SeMe)₃}]⁺ 417. IR (cm⁻¹): 2929 (w), 2267 (w), 1359 (s), 1092 (s), 991 (m), 835 (s), 727 (m), 614 (w), 559 (m), 447 (w).

[Cu{MeC(CH₂TeMe)₃}₂][PF₆] was prepared similarly to give a yellow solid (75%). Anal. Calcd for C₁₆H₃₆CuF₆PTe₆: C, 16.0; H, 3.0. Found: C, 15.9; H, 3.0. ¹H NMR (CDCl₃): δ 1.27 (s, 1H, CH₃C),

2.02 (s, 3H, TeCH₃), 2.98 (s, 2H, TeCH₂). ES⁺ (MeCN) *m/z*: 1058, 602, 563; calcd for [⁶³Cu{MeC(CH₂¹³⁰TeMe)₃}₂]⁺ 1071, [⁶³Cu{MeC(CH₂¹³⁰TeMe)₃}(NCMe)]⁺ 608, [⁶³Cu{MeC(CH₂¹³⁰TeMe)₃}]⁺ 567. IR (cm⁻¹): 2951 (w), 1360 (s), 1223 (w), 1090 (s), 991 (m), 841 (s), 728 (m), 610 (w), 558 (m), 477 (w).

[Cu{MeC(CH₂TePh)₃}₂][PF₆] was prepared similarly to give a yellow solid (44%). Anal. Calcd for C₄₆H₄₈CuF₆PTe₆: C, 35.1; H, 3.1. Found: C, 34.6; H, 2.2. ¹H NMR (CDCl₃): δ 1.25 (s, 1H, CH₃C), 3.13 (s, 2H, TeCH₂), 7.21–7.61 (m, 5H, TePh). ES⁺ (MeCN) *m/z*: 749; calcd for [⁶³Cu{MeC(CH₂¹³⁰TePh)₃}]⁺ 753. IR (cm⁻¹): 3050 (w), 2951 (w), 1572 (m), 1474 (m), 1433 (s), 1360 (s), 1261 (w), 1223 (w), 1095 (s), 1017 (m), 998 (m), 839 (s), 732 (s), 690 (s), 655 (w), 614 (w), 558 (m), 479 (w), 453 (w).

[Ag{MeC(CH₂SeMe)₃}₂][CF₃SO₃]. AgCF₃SO₃ (20 mg, 7.8 × 10⁻⁵ mol) was added to a solution of MeC(CH₂SeMe)₃ (56 mg, 1.6 × 10⁻⁴ mol) in dry CH₂Cl₂ (30 cm³), and the reaction mixture was stirred for 1 h. The solvent volume was reduced in vacuo to 5 cm³, and diethyl ether was added to give a white solid. Yield: 26 mg, 55%. Anal. Calcd for C₉H₁₈AgF₃O₃SSe₃: C, 17.8; H, 3.0. Found: C, 17.8; H, 2.7. ¹H NMR (CDCl₃): δ 1.29 (s, 1H, CH₃C), 2.29 (s, 3H, SeCH₃), 2.01 (s, 2H, SeCH₂). ES⁺ (MeCN) *m/z*: 808; calcd for [¹⁰⁷Ag{MeC(CH₂⁸⁰SeMe)₃}]⁺ 815. IR (cm⁻¹): 2962 (w), 2907 (w), 1410 (m), 1362 (s), 1274 (s), 1232 (m), 1162 (m), 1090 (s), 1037 (s), 990 (m), 908 (m), 835 (w), 760 (w), 643 (s), 557 (w), 524 (w).

[Ag{MeC(CH₂TeMe)₃}₂][CF₃SO₃] was prepared similarly to give a pale yellow, light-sensitive solid (63%). Anal. Calcd for C₁₇H₃₆AgF₃O₃STe₆: C, 16.3; H, 2.9. Found: C, 16.0; H, 2.1. ¹H NMR (CDCl₃): δ 1.30 (s, 1H, CH₃C), 2.18 (s, 3H, TeCH₃), 3.05 (s, 2H, TeCH₂). ES⁺ (MeCN) *m/z*: 1104, 609; calcd for [¹⁰⁷Ag{MeC(CH₂¹³⁰TeMe)₃}₂]⁺ 1115, [¹⁰⁷Ag{MeC(CH₂¹³⁰TeMe)₃}]⁺ 611. IR (cm⁻¹): 2951 (w), 2918 (w), 1362 (m), 1264 (s), 1233 (m), 1162 (m), 1095 (m), 1039 (m), 835 (m), 759 (w), 645 (s), 571 (w), 522 (w).

[Ag{MeC(CH₂TePh)₃}₂][CF₃SO₃] was prepared similarly to give a pale yellow, light-sensitive solid (29%). Anal. Calcd for C₄₇H₄₈AgF₃O₃STe₆·CH₂Cl₂: C, 33.7; H, 2.9. Found: C, 33.3; H, 2.8. ¹H NMR (CDCl₃): δ 1.23 (s, 1H, CH₃C), 2.39 (s, 2H, TeCH₂), 7.00–7.65 (m, 5H, TePh). ES⁺ (MeCN) *m/z*: 1477; calcd for [¹⁰⁷Ag{MeC(CH₂¹³⁰TePh)₃}₂]⁺ 1487. IR (cm⁻¹): 3063 (w), 2957 (w), 1572 (m), 1473 (m), 1432 (m), 1370 (m), 1263 (s), 1233 (m), 1161 (s), 1064 (w), 1039 (m), 1017 (m), 998 (m), 910 (w), 835 (w), 790 (w), 730 (s), 690 (s), 637 (s), 573 (w), 516 (w), 454 (m).

X-ray Crystallography. Crystallographic data are given in Table 1. The crystals were grown by vapor diffusion of diethyl ether into solutions of the complexes in acetone for [Pt{MeC(CH₂SeMe)₃}₂][PF₆]₂, in nitromethane for [Ru{MeC(CH₂SeMe)₃}₂][CF₃SO₃]₂, and in dichloromethane for [Ag{MeC(CH₂SeMe)₃}₂][CF₃SO₃]. Data collection used a Rigaku AFC7S four-circle diffractometer with graphite-monochromated Mo K α X-radiation ($\lambda = 0.71073 \text{ \AA}$). The structures were solved by heavy-atom Patterson methods¹⁸ and developed with iterative cycles of full-matrix least-squares refinement and difference Fourier syntheses.¹⁹ Some disorder was identified within the uncoordinated arms of the triselenoether ligands in [Pt{MeC(CH₂SeMe)₃}₂][PF₆]₂. Alternative sites were identified for C(15), Se(6), and C(16) with relative occupancies of 60:40, while within the other free arm, an alternative location was identified for C(8) with a 70:30 occupancy. This disorder model refined reasonably successfully.²⁰ All non-H atoms, except for the partially occupied C atoms, were refined anisotropically, and H atoms were placed in fixed, calculated positions (except for the H atoms associated with the disordered C atoms, which were not located and were omitted from the final structure factor calculation). For [Ru{MeC(CH₂SeMe)₃}₂][CF₃SO₃]₂ and [Ag{MeC(CH₂SeMe)₃}₂][CF₃SO₃], all non-H atoms were refined anisotropically, while H atoms were placed in fixed, calculated positions with $d(\text{C}-\text{H}) = 0.96 \text{ \AA}$.

(18) Beurskens, P. T.; Admiraal, G.; Beurskens, G.; Bosman, W. P.; Garcia-Granda, S.; Gould, R. O.; Smits, J. M. M.; Smykalla, C. *PATY, The DIRDIF Program System*. Technical Report of the Crystallography Laboratory; University of Nijmegen: Nijmegen, The Netherlands, 1992.

(19) *TeXsan: Crystal Structure Analysis Package*; Molecular Structure Corporation: The Woodlands, TX, 1995.

(20) Sheldrick, G. M. *Acta Crystallogr., Sect. A* **1990**, *46*, 467.

Table 1. Crystallographic Data

	[Pt{MeC(CH ₂ SeMe) ₃ } ₂][PF ₆] ₂	[Ru{MeC(CH ₂ SMe) ₃ } ₂][CF ₃ SO ₃] ₂	[Ag{MeC(CH ₂ SeMe) ₃ }][CF ₃ SO ₃]
formula	C ₁₆ H ₃₆ F ₁₂ P ₂ PtSe ₆	C ₁₈ H ₃₆ F ₆ O ₆ RuS ₈	C ₉ H ₁₈ AgF ₃ O ₃ SSe ₃
fw	1187.24	820.02	608.04
T, °C	-123	25	-123
space group	<i>P</i> 2 ₁ / <i>n</i>	<i>P</i> $\bar{1}$	<i>P</i> 2 ₁ / <i>n</i>
cryst syst	monoclinic	triclinic	monoclinic
a, Å	12.272(10)	8.658(3)	8.120(3)
b, Å	18.563(9)	11.533(3)	15.374(3)
c, Å	15.285(7)	8.659(2)	14.071(2)
α, deg	90	108.33(2)	90
β, deg	113.18(3)	91.53(3)	93.86(2)
γ, deg	90	106.01(2)	90
V, Å ³	3200(2)	782.8(4)	1752.6(7)
Z	4	1	4
ρ _{calcd} , g cm ⁻³	2.463	1.739	2.304
μ(Mo Kα), cm ⁻¹	113.69	11.02	75.27
R(F _o) ^a	0.054	0.048	0.046
R _w (F _o) ^b	0.049	0.050	0.060

$$^a R = \sum(|F_{\text{obs}}| - |F_{\text{calc}}|) / \sum |F_{\text{obs}}|. \quad ^b R_w = \sqrt{[\sum w_i (|F_{\text{obs}}| - |F_{\text{calc}}|)^2] / \sum w_i |F_{\text{obs}}|^2}.$$

Results and Discussion

Palladium and Platinum. The preparation of homoleptic selenoether and telluroether Pd(II) and Pt(II) complexes with tripodal ligands is of interest, since it may produce square planar complexes with a free donor atom available on both ligands, which may lead to the stabilization of different oxidation states. The target complexes [M(L³)₂][PF₆]₂ (M = Pd or Pt; L³ = MeC(CH₂SeMe)₃, MeC(CH₂TeMe)₃, or MeC(CH₂TePh)₃) were conveniently synthesized in moderate yield by the reaction of [MCl₂(NCMe)₂] with 2 molar equiv of ligand and TlPF₆ in MeCN. The selenoether complexes are stable in solution; however, the products containing MeC(CH₂TeMe)₃ appear to decompose in solution over a few hours. Coordination of selenium or tellurium to a metal center in these systems leads to chirality at the chalcogen. Coordinated ditelluroethers exist as two diastereoisomers, meso (with syn R groups) and DL (anti R groups).²¹ For the complexes [M(L-L)₂][PF₆]₂ (L-L = ditelluroether), the combinations of meso and DL result in five possible isomers (invertomers) containing eight distinct tellurium environments.⁵ These isomers may interconvert by pyramidal inversion at Te, a process whose energy depends on the metal, the ligand structure, the chelate ring size, and the ligands trans to Te.²¹ For the d⁸ complexes reported here, further complexity is anticipated from the presence of both free and coordinated donor groups. Despite this, the ¹H NMR spectra at 300 K for all six complexes were surprisingly simple, showing just one signal each for the EMe, CH₂, and MeC groups. This indicates that these complexes are probably fluxional in solution at room temperature, the dynamic processes involving the arms of the tripod rapidly flipping on and off the metal center. VT ¹H NMR studies were therefore conducted on these complexes. The spectra showed only a broadening of the resonances even at 180 K, indicating that fluxional processes were still occurring.

Variable-temperature ⁷⁷Se{¹H} and ¹²⁵Te{¹H} NMR studies were also undertaken. At 300 K, the ⁷⁷Se{¹H} spectra exhibited a broad feature at δ 110 and 114 for [Pd{MeC(CH₂SeMe)₃}₂][PF₆]₂ and [Pt{MeC(CH₂SeMe)₃}₂][PF₆]₂, respectively. At 220 K, these signals were significantly sharper, with w_{1/2} at ca. 30 Hz, indicating a slowing of the dynamic processes, although the low-temperature limiting spectra were not obtained. The Pd complex showed three signals at δ 157, 147 (coordinated Se),

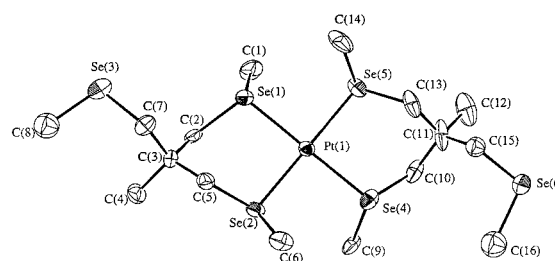


Figure 1. Structure of [Pt{MeC(CH₂SeMe)₃}₂]²⁺ with adopted numbering scheme. The figure shows the major conformation. Ellipsoids are drawn at the 40% probability level.

and 32 (uncoordinated Se). The Pt complex gave more information, showing five signals at δ 150, 149, 143, 142, and 34. The signals corresponding to coordinated Se are of similar intensity, probably indicating the up-up-up-down invertomer. The ¹⁹⁵Pt NMR spectrum for this complex at 220 K showed a major signal at δ -4630 and a minor signal at δ -4888; this compares with -4750 for [Pt([16]aneSe₄)₂]²⁺ ([16]aneSe₄ = 1,5,9,13-tetraselenacyclohexadecane) and -4677 for [Pt(MeSe(CH₂)₃SeMe)₂]²⁺, and it is therefore consistent with a Se₄ donor set at Pt(II).²² Coupling to ¹⁹⁵Pt is within the line width of the resonances.

The complexes [M{MeC(CH₂TePh)₃}₂][PF₆]₂ (M = Pd or Pt) showed no signals in the ¹²⁵Te{¹H} spectra at room temperature, although broad signals were observed at 190 K. No signals were observed at either 300 or 190 K for the complexes [M{MeC(CH₂TeMe)₃}₂][PF₆]₂ (M = Pd or Pt) in the ¹²⁵Te{¹H} or ¹⁹⁵Pt NMR spectra.

Crystals of the complex [Pt{MeC(CH₂SeMe)₃}₂][PF₆]₂ were grown from the vapor diffusion of diethyl ether into a solution of the complex in acetone. The structure (Figure 1 and Table 2) reveals a square planar Se₄ donor set around the Pt(II) metal center with the methyl groups on both ligands adopting a DL configuration and the uncoordinated arm of each tripod pointing away from, and thus not interacting with, the Pt(II) center, on opposite sides of the metal. The d(Pt-Se)'s (2.426(2), 2.430(2), 2.435(2), and 2.425(2) Å) are slightly longer than those observed for [Pt([16]aneSe₄)₂]²⁺ and [Pt{MeSe(CH₂)₃-SeMe)₂]²⁺.^{22,23} The angles around the central Pt atom do not

(22) Champness, N. R.; Kelly, P. F.; Levason, W.; Reid, G.; Slawin, A. M. Z.; Williams, D. J. *Inorg. Chem.* **1995**, *34*, 651-657.

(23) Champness, N. R.; Levason, W.; Quirk, J. J.; Reid, G. *Polyhedron* **1995**, *14*, 2753-2758.

(21) Abel, E. W.; Orrell, K. G.; Scanlan, S. P.; Stevenson, D.; Kemmitt, T.; Levason, W. *J. Chem. Soc., Dalton Trans.* **1991**, 591-595.

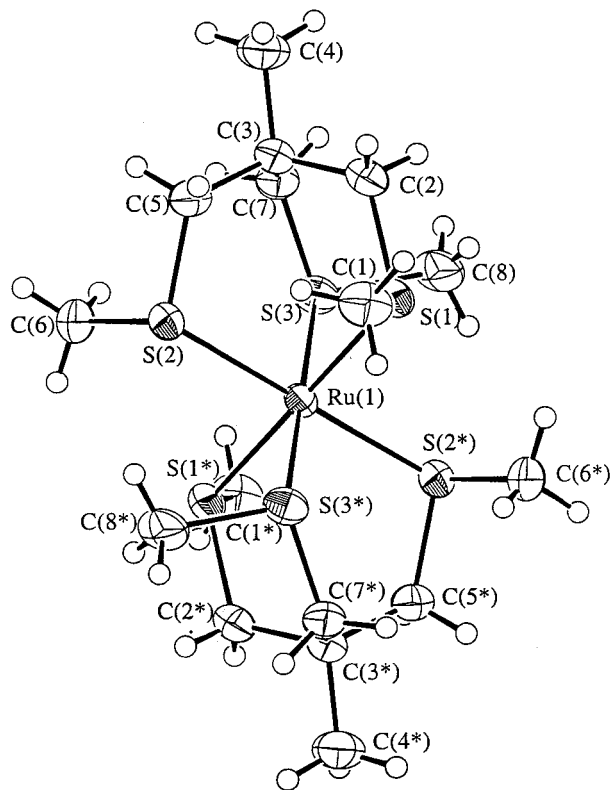
Table 2. Selected Bond Lengths (Å) and Angles (deg) for $[\text{Pt}\{\text{MeC}(\text{CH}_2\text{SeMe})_3\}_2]^{2+}$

atom	atom	distance	
Pt(1)	Se(1)	2.426(2)	
Pt(1)	Se(2)	2.430(2)	
Pt(1)	Se(4)	2.425(2)	
Pt(1)	Se(5)	2.435(2)	
atom	atom	atom	angle
Se(1)	Pt(1)	Se(2)	90.40(7)
Se(1)	Pt(1)	Se(4)	179.66(5)
Se(1)	Pt(1)	Se(5)	89.03(7)
Se(2)	Pt(1)	Se(4)	89.58(7)
Se(2)	Pt(1)	Se(5)	177.51(5)
Se(4)	Pt(1)	Se(5)	91.01(7)

deviate significantly from 90° or 180° , reflecting the good match of the six-membered chelate rings formed by the ligand and the cis angles required for the square planar geometry. The very flexible nature of the uncoordinated arms is also apparent from the crystal structure, which shows disorder in this region due to the presence of different conformations.

Ruthenium. Recently, we reported the synthesis of the first hexaseleno- and hexatelluroether complexes, $[\text{Ru}(\text{L}^3)_2][\text{CF}_3\text{SO}_3]_2$ ($\text{L}^3 = \text{MeC}(\text{CH}_2\text{EMe})_3$ where $\text{E} = \text{Se}$ or Te) along with the crystal structure of the selenoether complex.¹¹ We also noted from the electronic spectra that the Se_6 and Te_6 donor sets in these systems impose unusually strong ligand fields. We can now report the syntheses of the complexes $[\text{Ru}(\text{L}^3)_2][\text{CF}_3\text{SO}_3]_2$ ($\text{L}^3 = \text{MeC}(\text{CH}_2\text{SMe})_3$ or $\text{MeC}(\text{CH}_2\text{TePh})_3$), prepared by the reaction of 2 molar equiv of ligand with $[\text{Ru}(\text{dmf})_6][\text{CF}_3\text{SO}_3]_3$ in refluxing methanol. The electrospray mass spectra show peaks with the correct isotopic distribution for the doubly charged species $[\text{Ru}(\text{L}^3)_2]^{2+}$, and IR spectra show peaks associated with the coordinated ligands and the CF_3SO_3^- anions. Analysis of the electronic spectrum for the thioether complex gives 10 Dq at ca. $26\,500\text{ cm}^{-1}$ and B at ca. 260 cm^{-1} ; thus, the ligand field strength falls between those for $[\text{Ru}\{\text{MeC}(\text{CH}_2\text{SeMe})_3\}_2]^{2+}$ and $[\text{Ru}(\text{9}]\text{aneS}_3)_2]^{2+}$.

The $^{125}\text{Te}\{\text{H}\}$ NMR spectrum for the telluroether complex $[\text{Ru}\{\text{MeC}(\text{CH}_2\text{TePh})_3\}_2][\text{CF}_3\text{SO}_3]_2$ showed one peak at $\delta\ 481$, attributed to the syn isomer, since pyramidal inversion at the $\text{Ru}-\text{TeR}_2$ unit is expected to be slow.^{7,24} This behavior is similar to that observed previously for $[\text{Ru}\{\text{MeC}(\text{CH}_2\text{EMe})_3\}_2][\text{CF}_3\text{SO}_3]_2$ ($\text{E} = \text{Se}$ or Te). However, since for these complexes the homoleptic donor set affects the inversion barriers, VT ^1H NMR studies were conducted on the complex $[\text{Ru}\{\text{MeC}(\text{CH}_2\text{SeMe})_3\}_2][\text{CF}_3\text{SO}_3]_2$. No change in the spectrum was observed as the temperature was lowered to 180 K, indicating that these complexes are not undergoing fast inversion on the ^1H NMR time scale. The crystal structure of $[\text{Ru}\{\text{MeC}(\text{CH}_2\text{SMe})_3\}_2][\text{CF}_3\text{SO}_3]_2$ (Figure 2 and Table 3) shows this compound to be isostructural with $[\text{Ru}\{\text{MeC}(\text{CH}_2\text{SeMe})_3\}_2][\text{CF}_3\text{SO}_3]_2$, revealing an ordered centrosymmetric cation with the Ru occupying a crystallographic inversion center and coordinated to two tridentate, facially bound thioether ligands. The complex cation adopts the syn configuration with the Me substituents adopting a propeller-like arrangement. The $d(\text{Ru}-\text{S})$'s (2.375(2), 2.373(2), and 2.367(2) Å) are slightly longer than those for $[\text{Ru}(\text{9}]\text{aneS}_3)_2$, $d(\text{Ru}-\text{S}) = 2.3272(14)-2.3357(14)$ Å, probably due to the superior ligand properties of the macrocyclic ligand.²⁵ The $\text{S}-\text{Ru}-\text{S}$ bond angles involved in the six-membered chelate rings are very close to 90° .

**Figure 2.** Structure of $[\text{Ru}\{\text{MeC}(\text{CH}_2\text{SMe})_3\}_2]^{2+}$ with adopted numbering scheme. Ellipsoids are drawn at the 40% probability level.**Table 3.** Selected Bond Lengths (Å) and Angles (deg) for $[\text{Ru}\{\text{MeC}(\text{CH}_2\text{SMe})_3\}_2]^{2+}$

atom	atom	distance	
Ru(1)	S(1)	2.375(2)	
Ru(1)	S(2)	2.373(2)	
Ru(1)	S(3)	2.367(2)	
atom	atom	atom	angle
S(1)	Ru(1)	S(2)	88.81(6)
S(1)	Ru(1)	S(3)	87.52(6)
S(2)	Ru(1)	S(3)	89.84(6)

An important feature is the relative ease of formation of these homoleptic Ru complexes using the tripodal ligands. All previously reported seleno- and telluroether Ru(II) complexes have incorporated co-ligands such as halides, of macrocyclic ligands.

Rhodium and Iridium. As part of our study of 2:1 ditelluroether:metal species, we reported the complexes $[\text{Rh}(\text{L-L})_2\text{Cl}_2][\text{PF}_6]$ ($\text{L-L} = \text{RTe}(\text{CH}_2)_3\text{TeR}$ ($\text{R} = \text{Me}$ or Ph) or $o\text{-C}_6\text{H}_4(\text{TeMe})_2$), formed in high yield from the reaction of $\text{RhCl}_3 \cdot 3\text{H}_2\text{O}$ with L-L .⁷ We were therefore interested in establishing whether we could form stable hexaseleno- or hexatelluroether Rh(III) complexes using the tripodal ligands, without the use of halide co-ligands. Hexaseleno- and hexatelluroether coordination at rhodium and iridium centers has not been achieved previously.

The reaction of $[\text{Rh}(\text{OH})_2]^{3+}$ with 2 molar equiv of $\text{MeC}(\text{CH}_2\text{SeMe})_3$ and the addition of excess NH_4PF_6 affords $[\text{Rh}\{\text{MeC}(\text{CH}_2\text{SeMe})_3\}_2][\text{PF}_6]_3$ as a red powder. The IR spectrum indicated the presence of the coordinated ligand and the

(24) Levason, W.; Quirk, J. J.; Reid, G.; Smith, S. M. *J. Chem. Soc., Dalton Trans.* **1997**, 3719–3724.

(25) Bell, M. N.; Blake, A. J.; Schröder, M.; Küppers, H.-J.; Wieghardt, K. *Angew. Chem., Int. Ed. Engl.* **1987**, 26, 250–251.

anion PF_6^- , and the ^1H NMR spectrum gave a complex pattern indicating the presence of a number of invertomers. The electrospray mass spectrum gave one cluster of peaks centered at $m/z = 395$, which corresponds to the $[\text{Rh}\{\text{MeC}(\text{CH}_2\text{SeMe})_3\}\{\text{MeC}(\text{CH}_2\text{SeMe})_2(\text{CH}_2\text{Se})\}]^{2+}$ ion, therefore indicating that dealkylation of the tripositive cation occurred during ionization to produce the dipositive cation. The isotope pattern confirmed this assignment, matching well with the calculated pattern. The $^{77}\text{Se}\{^1\text{H}\}$ NMR spectrum at 300 K showed several resonances, but these did not show any coupling to ^{103}Rh ; therefore, the sample was cooled to 200 K, whereupon doublets were observed in the range δ 126–159, with $^1J_{\text{Rh}-\text{Se}}$ at approximately 43 Hz. The Rh–Se coupling constant is consistent with related complexes such as *trans*- $[\text{RhCl}_2\{[8]\text{aneSe}_2\}][\text{BF}_4]$ ($[8]\text{aneSe}_2 = 1,5$ -diselenacyclooctane; 42 Hz) and *cis*- $[\text{RhCl}_2\{[16]\text{aneSe}_4\}][\text{PF}_6]$ (36 Hz, 37 Hz).²⁶

Attempts to prepare the related telluroether complexes were unsuccessful, probably due to facile decomposition or dealkylation occurring. These have been observed for other systems.²⁷

The yellow Ir(III) complex $[\text{Ir}\{\text{MeC}(\text{CH}_2\text{SeMe})_3\}_2][\text{PF}_6]_3$ was prepared by the reaction of $\text{MeC}(\text{CH}_2\text{SeMe})_3$ with the Ir(I) precursor $[\text{IrCl}(\text{C}_8\text{H}_{14})_2]_2$, via the oxidation of Ir(I) by HBF_4 . Interestingly, similar reaction conditions using the ligand [9]-aneS₃ gave the hydride complex $[\text{IrH}(\text{[9]aneS}_3)_2][\text{BF}_4]_2$, which can be converted to $[\text{Ir}(\text{[9]aneS}_3)_2]^{3+}$ by treatment with HNO_3 .²⁸ The ^1H NMR spectrum indicated the presence of the ligand, and the IR spectrum showed bands assigned to the ligand and PF_6^- anion. Interestingly, the electrospray mass spectrum showed the same behavior as the rhodium complex, one cluster of peaks corresponding to the $[\text{Ir}\{\text{MeC}(\text{CH}_2\text{SeMe})_3\}\{\text{MeC}(\text{CH}_2\text{SeMe})_2(\text{CH}_2\text{Se})\}]^{2+}$ ion at $m/z = 439$. Therefore, dealkylation has again occurred during the ionization process. The $^{77}\text{Se}\{^1\text{H}\}$ NMR spectrum showed several peaks at δ 77.6, 87.4, and 109.1, entirely reasonable shifts compared to those of the previous complexes. Like the rhodium complexes, the analogous telluroether complexes could not be prepared under these reaction conditions.

Copper and Silver. A range of homoleptic dithio-, diseleno-, and ditelluroether complexes with Cu(I) and Ag(I) metal centers have been reported.¹⁰ The crystal structures of several of these compounds revealed highly unusual structural features, including a three-dimensional infinite lattice for the complex $[\text{Ag}_n(\text{PhSCH}_2\text{CH}_2\text{CH}_2\text{SPh})_{2n}]^{n+}$.²⁹ Therefore, as part of this study, we decided to investigate the coordination chemistry of the tripodal ligands with Cu(I) and Ag(I) ions.

The reaction of $[\text{Cu}(\text{NCMe})_4][\text{PF}_6]$ with 2 molar equiv of L^3 ($\text{L}^3 = \text{MeC}(\text{CH}_2\text{SeMe})_3$, $\text{MeC}(\text{CH}_2\text{TeMe})_3$, or $\text{MeC}(\text{CH}_2\text{TePh})_3$) gave the $[\text{Cu}(\text{L}^3)_2][\text{PF}_6]$ species as pale yellow products. The electrospray mass spectra showed peaks corresponding to the $[\text{Cu}(\text{L}^3)]^+$ ion for all complexes; however, the $[\text{Cu}(\text{L}^3)_2]^+$ ion was only observed for the $\text{MeC}(\text{CH}_2\text{TeMe})_3$ complex. This behavior is common for other systems.⁸ Elemental analyses confirmed the identity of the products as the bis ligand species. The ^1H NMR spectra were rather uninformative, showing only the presence of the coordinated ligand, indicating that rapid exchange processes such as reversible intramolecular chelate ring-opening and pyramidal inversion are probably occurring

in solution. Similar behavior was observed for the bis bidentate complexes, for example, $[\text{Cu}\{\text{MeSeCH}_2\text{CH}_2\text{SeMe}\}_2][\text{PF}_6]_8$. Attempts to obtain ^{63}Cu , $^{77}\text{Se}\{^1\text{H}\}$, and $^{125}\text{Te}\{^1\text{H}\}$ NMR data were unsuccessful even at low temperature, again illustrating the rapid dynamic behavior of these complexes in solution.

Recently, the structures of Ag(I) complexes with thioether cages³⁰ and the tripodal phosphine, $\text{CH}_3\text{C}(\text{CH}_2\text{PPh}_2)_3$, have been reported.³¹ This, together with the structures previously identified by us for the bidentate group 16 ligand complexes of Ag(I) and Cu(I),²⁹ prompted us to investigate the coordination chemistry of the group 16 tripod ligands with Ag(I). The reaction of 2 molar equiv of L^3 ($\text{L}^3 = \text{MeC}(\text{CH}_2\text{SeMe})_3$, $\text{MeC}(\text{CH}_2\text{TeMe})_3$, or $\text{MeC}(\text{CH}_2\text{TePh})_3$) with $\text{Ag}[\text{CF}_3\text{SO}_3]$ gave white, light-sensitive powders after the reduction of the solvent in vacuo and the addition of diethyl ether.

The ^1H NMR spectra of the Ag(I) complexes showed behavior similar to that of the Cu(I) compounds and provided little structural information. Elemental analyses gave information on the stoichiometry, revealing that although the telluroether complexes are the expected $[\text{Ag}\{\text{MeC}(\text{CH}_2\text{TeMe})_3\}_2][\text{CF}_3\text{SO}_3]$ and $[\text{Ag}\{\text{MeC}(\text{CH}_2\text{TePh})_3\}_2][\text{CF}_3\text{SO}_3]$ complexes, the selenoether product is in fact the 1:1 complex, $[\text{Ag}\{\text{MeC}(\text{CH}_2\text{SeMe})_3\}][\text{CF}_3\text{SO}_3]$. The electrospray mass spectra of all three complexes showed peaks corresponding to the $[\text{Ag}(\text{L}^3)]^+$ ion. Unfortunately, we were again unable to obtain the $^{77}\text{Se}\{^1\text{H}\}$ or the $^{125}\text{Te}\{^1\text{H}\}$ NMR spectra. However, since the crystal structures of the bidentate group 16 complexes revealed extended structures, we were particularly interested in the structures of these complexes. Colorless crystals of the selenoether complex $[\text{Ag}\{\text{MeC}(\text{CH}_2\text{SeMe})_3\}][\text{CF}_3\text{SO}_3]$ were grown by vapor diffusion of diethyl ether into a 2 molar equiv solution of $\text{MeC}(\text{CH}_2\text{SeMe})_3$ and 1 molar equiv of $\text{Ag}(\text{CF}_3\text{SO}_3)$ in dry CH_2Cl_2 under a N_2 atmosphere. The structure of $[\text{Ag}\{\text{MeC}(\text{CH}_2\text{SeMe})_3\}][\text{CF}_3\text{SO}_3]$ shows an extended chain (Figure 3 and Table 4) via bidentate coordination of $\text{MeC}(\text{CH}_2\text{SeMe})_3$ to one Ag(I) and monodentate coordination to an adjacent Ag(I), resulting in a distorted trigonal planar geometry around each Ag atom. The electrospray mass spectrum of these crystals was identical to that of the bulk solid, giving a cluster of peaks for $[\text{Ag}\{\text{MeC}(\text{CH}_2\text{SeMe})_3\}_2]^+$. This species may be expected as a fragment of the crystallographically identified linear chain polymer involving a 1:1 Ag:selenoether ratio, since the selenoether ligands are effectively bridging Ag ions. The $d(\text{Ag}-\text{Se})$'s (2.544(1), 2.607(2), and 2.678(1) Å) vary by more than 0.1 Å, where the two longer bonds are in the chelate, due to the nature of the extended structure. Similar behavior was observed for $[\text{Ag}_n\{\mu\text{-}o\text{-C}_6\text{H}_4(\text{SeMe})_2\}_n\{\mu\text{-}o\text{-C}_6\text{H}_4(\text{SeMe})_2\}_n]^{n+}$ where bond lengths varied from 2.587(1) to 2.861(1) Å.¹⁰ However the Ag–Se bond distances are comparable to those observed for $[\text{Ag}(\text{MeSeCH}_2\text{CH}_2\text{SeMe})_2]\text{BF}_4$ ($d(\text{Ag}-\text{Se}) = 2.610(1)$ – $2.638(1)$ Å).⁹ The Se–Ag–Se bond angle involved in the six-membered chelate ring is $94.36(4)^\circ$, with the two angles of the Se attached to the next ligand at $126.09(5)^\circ$ and $139.55(5)^\circ$, and the Me substituents were again oriented in the syn configuration.

Electrochemistry. The electrochemical behavior of all the platinum group metal complexes was investigated by cyclic voltammetry over the range of +1.8 to –1.8 V in MeCN solution at room temperature. The redox responses were rather uninformative, revealing only very broad, irreversible processes the potentials of which shift when the scan rate is varied. The

(26) Levason, W.; Quirk, J. J.; Reid, G. *J. Chem. Soc., Dalton Trans.* **1996**, 3713–3719.

(27) Kemmitt, T.; Levason, W.; Spicer, M. D.; Webster, M. *Organometallics* **1990**, *9*, 1181–1184.

(28) Blake, A. J.; Gould, R. O.; Holder, A. J.; Hyde, T. I.; Reid, G.; Schröder, M. *J. Chem. Soc., Dalton Trans.* **1990**, 1759–1764.

(29) Black, J. R.; Champness, N. R.; Levason, W.; Reid, G. *J. Chem. Soc., Chem. Commun.* **1995**, 1277–1278.

(30) Alberto, R.; Angst, D.; Abram, U.; Ortner, K.; Kaden, T. A.; Schubiger, A. P. *J. Chem. Soc., Chem. Commun.* **1999**, 1513–1514.

(31) James, S. T.; Mings, D. M. P.; White, A. J. P.; Williams, D. J. *J. Chem. Soc., Chem. Commun.* **1998**, 2323–2324.

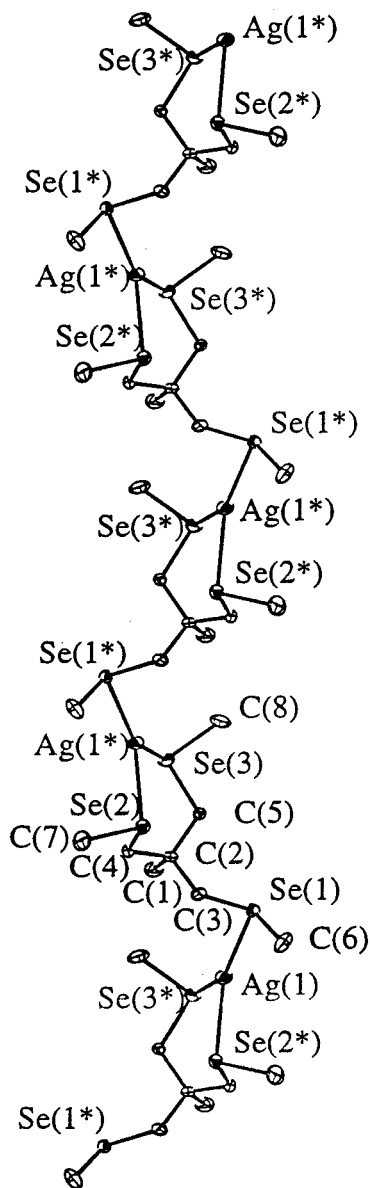


Figure 3. Structure of a portion of the infinite chain adopted by $[\text{Ag}\{\text{MeC}(\text{CH}_2\text{SeMe})_3\}]^+$ with adopted numbering scheme. Ellipsoids are drawn at the 40% probability level.

absence of any reversible redox processes for the Ru(II) complexes is in accord with the large ligand field splittings observed for these species.

Table 4. Selected Bond Lengths (Å) and Angles (deg) for $[\text{Ag}\{\text{MeC}(\text{CH}_2\text{SeMe})_3\}]^+$

atom	atom	distance	
Ag(1)	Se(1)	2.544(1)	
Ag(1)	Se(2*)	2.678(1)	
Ag(1)	Se(3*)	2.607(2)	
atom	atom	atom	angle
Se(1)	Ag(1)	Se(2*)	126.09(5)
Se(1)	Ag(1)	Se(3*)	139.55(5)
Se(2*)	Ag(1)	Se(3*)	94.36(4)

Conclusion

This study has illustrated the versatility of the group 16 tripod ligands, $\text{MeC}(\text{CH}_2\text{SeMe})_3$, $\text{MeC}(\text{CH}_2\text{TeMe})_3$, and $\text{MeC}(\text{CH}_2\text{TePh})_3$, with a variety of medium oxidation-state transition metal ions. In particular, the variety of coordination modes that they may adopt as a consequence of metal ion requirements has been demonstrated. For the Ru(II), Rh(III), and Ir(III) complexes, facial tridentate coordination, the Pd(II) and Pt(II) bidentate coordination with one free arm of the ligand, is observed, and for the Ag(I) selenoether complex, both bi- and monodentate coordination to two different Ag(I) centers are observed. The homoleptic selenoether and telluroether coordination of the complexes in this work contrasts with the much more familiar halo derivatives of the platinum metal ions. The fact that the telluroether complexes could not be isolated for Rh(III) and Ir(III) is perhaps more a consequence of the harsh reaction conditions avoiding halide coordination than of the stability of the final complexes. Alternative routes to Rh(I) and Ir(I) selenoether and telluroether compounds are under investigation.

Acknowledgment. The authors thank the EPSRC for financial support (SDO) and Johnson Matthey plc for generous loans of platinum metal salts.

Supporting Information Available: X-ray crystallographic files in CIF format for the structure determinations of $[\text{Pt}\{\text{MeC}(\text{CH}_2\text{SeMe})_3\}_2][\text{PF}_6]_2$, $[\text{Ru}\{\text{MeC}(\text{CH}_2\text{SeMe})_3\}_2][\text{CF}_3\text{SO}_3]_2$, and $[\text{Ag}\{\text{MeC}(\text{CH}_2\text{SeMe})_3\}][\text{CF}_3\text{SO}_3]$. This material is available free of charge via the Internet at <http://pubs.acs.org>.